AIP Applied Physics Letters

Investigating the improvement of resistive switching trends after post-forming negative bias stress treatment

Hsueh-Chih Tseng, Ting-Chang Chang, Jheng-Jie Huang, Po-Chun Yang, Yu-Ting Chen, Fu-Yen Jian, S. M. Sze, and Ming-Jinn Tsai

Citation: Applied Physics Letters **99**, 132104 (2011); doi: 10.1063/1.3645004
View online: http://dx.doi.org/10.1063/1.3645004
View Table of Contents: http://scitation.aip.org/content/aip/journal/apl/99/13?ver=pdfcov
Published by the AIP Publishing

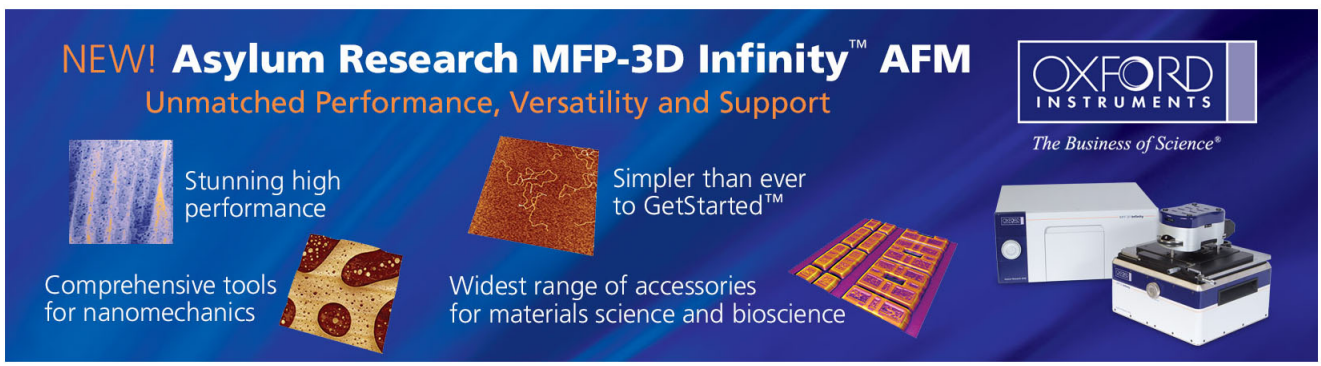

Investigating the improvement of resistive switching trends after post-forming negative bias stress treatment

Hsueh-Chih Tseng,[1] Ting-Chang Chang,[1,2,a)] Jheng-Jie Huang,[1] Po-Chun Yang,[3] Yu-Ting Chen,[3] Fu-Yen Jian,[4] S. M. Sze,[1,4,5] and Ming-Jinn Tsai[6]
[1]*Department of Physics, National Sun Yat-Sen University, Kaohsiung 804, Taiwan*
[2]*Center for Nanoscience and Nanotechnology, National Sun Yat-Sen University, Kaohsiung 804, Taiwan*
[3]*Department of Electro-Optical Engineering, National Sun Yat-Sen University, Kaohsiung 804, Taiwan*
[4]*Institute of Electronics, National Chiao Tung University, Hsinchu 300, Taiwan*
[5]*Department of Electrical Engineering, Stanford University, Stanford, California 94305-4085, USA*
[6]*Electronics and Optoelectronics Research Laboratory, Industrial Technology Research Institute, Chutung, Hsinchu 310, Taiwan*

(Received 22 May 2011; accepted 3 September 2011; published online 29 September 2011)

This paper investigates the improvement of resistive switching trends after post-forming negative bias stress treatment of a Pt/Yb_2O_3/TiN device that has undergone positive bias forming process for activation. After the treatment, characteristics of the conductive filament, such as the temperature dependence of resistivity and transition mechanism, undergo changes. Furthermore, this treatment causes the conductive filament to transform from being primarily composed of vacancies to being metallic Yb dominant, which not only reduces operation voltages such as V_{set} and V_{reset} but also improves the on/off ratio. In reliability tests, the device has stable retention. © *2011 American Institute of Physics*. [doi:10.1063/1.3645004]

Resistive random access memory (RRAM) has attracted considerable interest for the next generation of nonvolatile memory devices due to its simple structure, low operation voltage, and process compatibility with the current complementary metal-oxide-semiconductor (CMOS) industry.[1] Up to now, two dominant resistance switching mechanisms have been proposed. One is oxygen vacancy nucleation at a metal/oxide interface.[2,3] The other mechanism is the conductive filament (CF) model, which describes the formation/rupture of a metallic filament using a metal such as Cu or Ag to act as mobile ions in the oxide.[4] Recently, rare earth (RE) metal oxides, which are used as a high-k gate insulator for advanced CMOS technology,[5,6] have exhibited resistance switching phenomena.[7,8] One of the RE metal oxides, ytterbium oxide (Yb_2O_3), is attractive as a gate dielectric in CMOS devices because of its dielectric constant of 15, larger energy band gap (>5 eV), and predicted chemical and thermal stability with Si. Therefore, it also has been explored for semiconductor applications including memory devices, logical devices, and optoelectronic devices.[9] The application of Yb_2O_3 in the resistive switching field, however, has not been sufficiently researched.

This work investigates the bipolar resistance switching characteristics of a Pt//Yb_2O_3/TiN structure by using an additional negative bias stress (NBS) treatment after the positive electroforming (PF) process which is necessary to activate the RRAM device and which causes the resistance state (RS) transformation to be switchable. The power law relationship of the low resistance state (LRS) indicates that the NBS treatment can change the transition mechanism; moreover, further confirmation of this can be found in the temperature dependence of LRS trends. In addition, a mechanism is proposed to explain the influence of the presence or absence of NBS treatment on resistive switching characteristics of Yb_2O_3 based RRAM of the device.

Yb_2O_3 thin film of 20 nm thickness was deposited on a TiN/Si substrate by reactive magnetron RF sputtering an Yb_2O_3 target in Ar (30 SCCM) ambient at room temperature. Then the Pt top electrode (TE) was deposited and patterned by the liftoff process. The without-NBS device was only PF treated, whereas the with-NBS device was used as a reference with NBS treatment after the PF activation and will be referred to as without-NBS and with-NBS devices hereafter. All electrical characteristics were measured over an 8 μm × 8 μm cell size by an Agilent B1500 semiconductor parameter analyzer. During these measurements, bias was applied to the TiN bottom electrode (BE) while the Pt TE was ground.

The transition between LRS and high resistance state (HRS) of the without-NBS and the with-NBS devices was observed by using the same dc voltage sweeping mode, as shown in Fig. 1. During the PF process, as shown in the inset (i) of Fig. 1(a), a positive dc bias of about 12 V was applied to BE with a current compliance of 1 μA. Figure 1(a) shows that the resistance of the without-NBS device can be switched to HRS by applying negative bias of about −2 V. In a subsequent sweep, the RS can be switched again to LRS by applying a predetermined positive bias of about 2 V with a 10 mA current compliance. During the NBS treatment, a higher and reverse polarity dc bias with a 10 mA current compliance was applied to the without-NBS device, as shown in Fig. 1(a). First, when the bias increased to about −3 V, there was a first obvious transformation in RS, which suddenly transformed from LRS to NBS-$HRS_{initial}$ (after the NBS treatment of first transformation without bipolar switching operation) and caused the local CF narrowing due to the joule heating effect.[10] Subsequently, as the bias continued to increase at about −5 V, the RS

a)Author to whom correspondence should be addressed. Electronic mail: tcchang@mail.phys.nsysu.edu.tw.

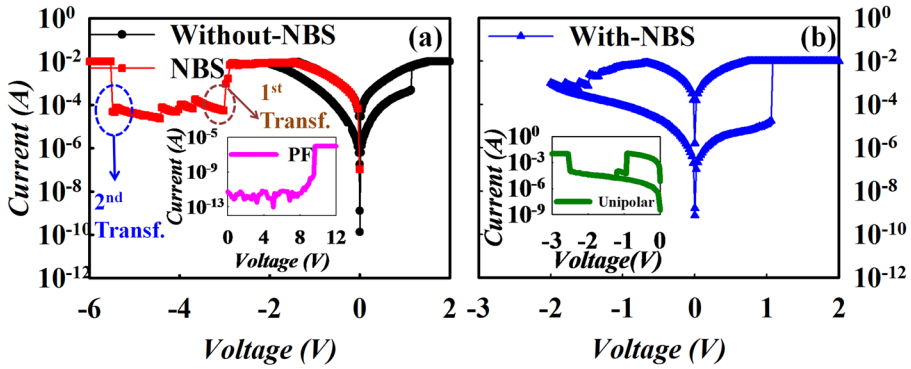

FIG. 1. (Color online) (a) The I-V curve characteristics of the without-NBS sample and with-NBS treatment. The inset shows the PF treatment. (b) The I-V curve characteristics for the control sample. The inset shows unipolar characteristics. Both (a) and (b) show typical I-V curve characteristics with 10 mA compliance.

transformed again from the NBS-HRS$_{initial}$ to NBS-LRS$_{initial}$ (after the NBS treatment of second transformation without bipolar switching operation), which is similar to the forming process and reconstructs the CF. Figure 1(b) shows the different trend of bipolar resistive switching characteristic of the with-NBS device, different from the without-NBS device. In addition, a few cycles of unipolar switching phenomena appear momentarily, as shown in the inset of Fig. 1(b).

The inset (i) of Fig. 2 shows that the LRS$_{initial}$ (after PF treatment without bipolar switching operation) of the without-NBS device decreases when the ambient temperature increases, as is typical of semiconductor behavior properties.[11] This implies that the CF is the dominated by vacancies.[12] In contrast, under the second RS transformation of the NBS treatment, the oxygen vacancies and oxygen ions can be re-generated. Because the number of the re-generated oxygen vacancies and diffusion ions are enough to cause the metallic CF formation, the NBS-LRS$_{initial}$ of the with-NBS device increases as ambient temperature rises, which indicates typical metallic behavior;[11] furthermore, calculating the temperature coefficient of the resistance α indicates that α is about 9.74×10^{-4} K^{-1} (the ideal α of metallic Yb is about 1.3×10^{-3} K^{-1}), as shown in Fig. 2. This result indicates that the NBS treatment can generate the Yb metallic-type conductive path(s). However, these mobile oxygen ions drift to Pt and can be chemisorbed at the grain boundary or penetrate through the Pt layer during the NBS treatment.[13,14] After bipolar stressing (switching), these mobile oxygen ions cannot fully drift back to the insulator and towards TiN;[15]

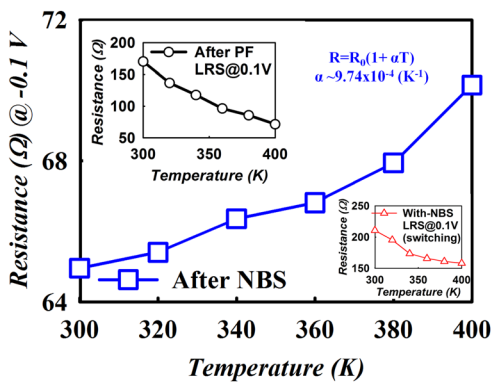

FIG. 2. (Color online) The temperature-dependent initial low resistance state in with-NBS samples without switching operation, the inset (i) without-NBS device and the inset (ii) with-NBS with the bipolar switching operation.

moreover, the CF characteristic changes from metallic behavior to semi-like behavior, as shown in the inset (ii) of Fig. 2, because the decrease in mobile oxygen ions acts to reconstruct the thinner redox reaction region during the bipolar-set process.

Figure 3 shows the power law relationship and current fitting between the without-NBS and with-NBS devices. According to the power law relationship ($I = KV^n$) for the I-V plot of LRS, the switching mechanism before and after NBS treatment is different. Fig. 3(a) shows that the value of n is about 1.78 for the without-NBS sample and about 1.22 for the with-NBS while both underwent the bipolar switching operation is due to the switching layer (SL) formation. However, after the NBS treatment without bipolar switching operation, the value of n was about 0.97. If no SL exists during the switching process, as in unipolar switching,[16] the n value would be about 1 due to the metallic filament formation. In addition, the current fitting results also show that the LRS for the without-NBS device obeys the Schottky conduction behavior due to the original-SL formation, as shown in Fig. 3(b). The NBS treatment can cause the original-SL disintegrating, which makes the LRS transition mechanism to follow the Ohmic conduction behavior (the slope is 1.0), as shown in Fig. 3(c); furthermore, because the reconstructed

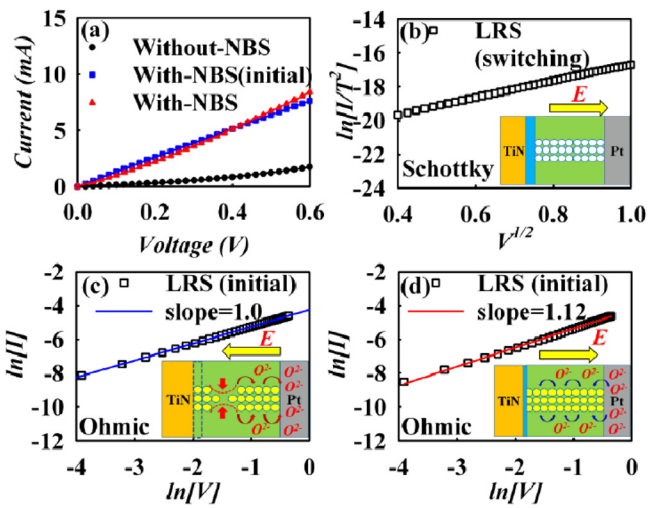

FIG. 3. (Color online) The LRS mechanism fitting result for (a) power law relationship, (b) Schottky mechanism of the without-NBS device, (c) Ohmic mechanism of the with-NBS without bipolar switching, and (d) Ohmic mechanism of the with-NBS with bipolar switching. And the inset of (b)–(d) shows the schematic diagram of the without-NBS and with-NBS mechanism.

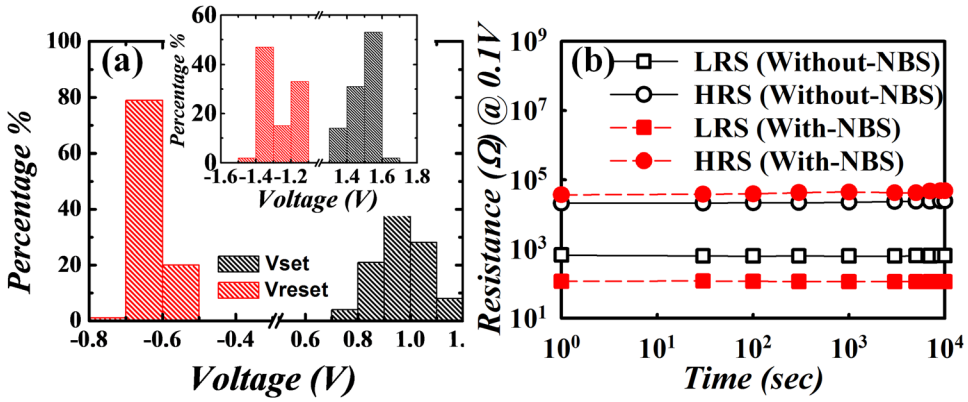

FIG. 4. (Color online) (a) Set and reset voltage statistics for with-NBS samples for 100 cycles in dc sweeping mode. The inset shows the statistics of the without-NBS sample. (b) Retention characteristics for both with and without NBS samples for both resistance states at 85 °C.

SL is thinner than the without-NBS device, the LRS transition mechanism also follows the Ohmic conduction behavior (the slope is 1.12), as shown in Fig. 3(d).

The comparisons in Fig. 4(a) show that the without-NBS device also has lower V_{set} and V_{reset}. The decrease in mobile oxygen ions of the with-NBS device can be easily induced the redox reaction for a smaller V_{set}, and the metallic CF of the with-NBS device has a better electric conductivity making the smaller V_{reset} induce the reset current. To test the device for practical memory application, reliability of retention was monitored. Figure 4(b) shows the data retention at 85 °C. The results reveal that the proposed treatment can retain stable HRS and LRS without degradation longer than 10^4 s.

In conclusion, the effect of NBS on the resistive switching characteristics of Pt/Yb_2O_3/TiN RRAM device has been investigated. Based on experimental results, the NBS treatment can transform the CF from vacancy-dominated to metallic Yb dominant. Hence, the characteristics of resistance switching mechanism can be changed into redox reaction accompanying joule heating effect by applying the NBS treatment in order to obtain better bipolar switching characteristics such as lower set and reset voltages and a larger on/off ratio.

This work was performed at National Science Council Core Facilities Laboratory for Nano-Science and Nano-Technology in Kaohsiung-Pingtung area and was supported by the National Science Council of the Republic of China under Contract Nos.NSC-100-2120-M-110-003 and NSC-97-2112-M-110-009-MY3.

[1]K. Szot, W. Speier, G. Bihlmayer, and R. Waser, Nature Mater. **5**(4), 312 (2006).
[2]J. J. Yang, F. Miao, M. D. Pickett, D. A. A. Ohlberg, D. R. Stewart, C. N. Lau, and R. S. Williams, Nanotechnology **20**, 215201 (2009).
[3]C. Yoshida, K. Kinoshita, T. Yamasaki, and Y. Sugiyama, Appl. Phys. Lett. **93**, 042106 (2008).
[4]C. Schindler, G. Staikov, and R. Waser, Appl. Phys. Lett. **94**, 072109 (2009).
[5]A. Fissel, M. Czernohorsky, and H. J. Osten, Superlattices Microstruct. **40**, 551 (2006).
[6]L. Marsella and V. Fiorentini, Phys. Rev. B **69**, 172103 (2004).
[7]X. Cao, X. Li, X. Gao, W. Yu, X. Liu, Y. Zhang, L. Chen, and X. Cheng, J. Appl. Phys. **106**, 073723 (2009).
[8]K. C. Liu, W. H. Tzeng, K. M. Chang, Y. C. Chan, C. C. Kuo, and C. W. Cheng, Microelectron. Reliab. **50**, 670 (2010).
[9]T. M. Pan and W. S. Huang, Appl. Surf. Sci. **255**, 4979 (2009).
[10]E. A. Miranda, C. Walczyk, C. Wenger, and T. Schroeder, IEEE Electron Device Lett. **31**(6), 609 (2010).
[11]C. Chen, Y. C. Yang, F. Zeng, and F. Pan, Appl. Phys. Lett. **97**, 083502 (2010).
[12]S. Y. Wang, D. Y. Lee, T. Y. Tseng, and C. Y. Lin, Appl. Phys. Lett. **95**, 112904 (2009).
[13]L. Goux, P. Czarnecki, Y. Y. Chen, L. Pantisano, X. P. Wang, R. Degraeve, B. Govoreanu, M. Jurczak, D. J. Wouters, and L. Altimime, Appl. Phys. Lett. **97**, 243509 (2010).
[14]L. Goux, X. P. Wang, Y. Y. Chen, L. Pantisano, N. Jossart, B. Govoreanu, J. A. Kittl, M. Jurczak, L. Altimime, and D. J. Wouters, Electrochem. Solid-State Lett. **14**(6), H244 (2011).
[15]S. Yu and H.-S. Philip Wong, IEEE Electron Device Lett. **31**(12), 1455 (2010).
[16]D.-H. Kwon, K. M. Kim, J. H. Jang, J. M. Jeon, M. H. Lee, G. H. Kim, X.-S. Li, G.-S. Park, B. Lee, S. Han, M. Kim, and C. S. Hwang, Nat. Nanotechnol. **5**, 148 (2010).